Mössbauer study of the high-temperature phase of Co-substituted magnetites, $Co_xFe_{3-x}O_4$. II. $x \geq 0.1$

R. M. Persoons,* E. De Grave, P. M. A. de Bakker, and R. E. Vandenberghe
Laboratory of Magnetism, University of Gent, Proeftuinstraat 86, B-9000 Gent, Belgium
(Received 13 March 1992; revised manuscript received 21 July 1992)

Transmission Mössbauer spectra at variable temperatures between 80 and 860 K have been collected for Co-substituted magnetities, $Co_xFe_{3-x}O_4$, with $x=0.1$, 0.2, and 0.4, and at two selected temperatures with the absorber in a longitudinal external magnetic field of 55 kOe. It is concluded that the interpretation of the spectra based on an earlier reported structural model leads to inconsistent results. An adequate and consistent description was obtained using a superposition of two model-independent hyperfine-field distributions, one arising from the tetrahedral (A) iron species, the second one from the octahedral (B) irons. The evaluated distributions clearly reveal the presence of two distinct B-site components, reflecting the existence of two different electronic states for the B-site irons at temperatures not exceeding ≈ 650 K. The appearance of two B sites is quantitatively explained on the basis of structural considerations. At high temperatures, one of the B-site components gradually disappears in favor of the other, indicating that all B-site irons become involved in the electron-exchange process. The behavior of the A-site center shifts suggests that these sites become involved in the electron-exchange process at temperatures approaching or exceeding the Curie temperature. The A-site hyperfine field is adequately described by a Brillouin function. The obtained values for the A-A (10.5±1 K) and A-B (21.5±1.0 K) superexchange integrals give no indication as to whether they depend on the Co concentration. The nonlocalized-electron model is unable to reproduce the temperature dependence of the octahedral hyperfine field. Spectra at selected temperatures were obtained for compositions $x=0.6$, 0.8, and 0.9. The A-site distributions are sharp and quite symmetric, whereas the shape of the B-site hyperfine-field distributions indicates the presence of more than two charge states for these iron species. For all considered compositions the magnetic order-disorder transition is sharp. The Curie temperature T_C slightly decreases with increasing Co content. For $x=0.1$, 0.2, and 0.4 the A-site electric-field gradient is close to zero, but not so for higher substitutions. The isomer shifts at a given temperature above T_C decrease with increasing x, reflecting the evolution towards pure Fe^{3+} states.

I. INTRODUCTION

In the first part (paper I) of this report on a comprehensive Mössbauer-spectroscopic study of Co-substituted magnetites, $Co_xFe_{3-x}O_4$, at temperatures T above the Verwey-transition temperature T_V, it was demonstrated that the presence of Co in the magnetite lattice, even in amounts as small as $x \leq 0.04$, is clearly reflected in the spectra and in the Mössbauer parameters derived from these. The observed features could be related either to the giant contribution of octahedral Co^{2+} to the magnetocrystalline anisotropy, which determines the direction of the easy axis of magnetization, or to the perturbing effects of the foreign Co ions on the electron exchange between Fe^{2+} and Fe^{3+} on the octahedral sites of the magnetite lattice.

Paper II, which is presented hereafter, is devoted to substitutions $x \geq 0.1$. In an earlier communication by two of the present authors,[1] it was shown that for x values 0.1, 0.2, and 0.4 the presence of a Verwey-like transition at $T=T_{VL}$ is reflected in the Mössbauer spectra. Since a Verwey transition does not take place according to the magnetostriction measurements[2] on the same samples, it was concluded that the transition concerns a locally confined phenomenon. This conclusion is consistent with the suggestion put forward in paper I concerning the effect of the Co substitution on the dual nature of the electron-exchange process as displayed in the temperature variation of the differential line broadening of the B-site absorption lines.

For $x=0.2$, the transition temperature T_{VL} was found to be 70±10 K. For the $x=0.4$ sample, a value for T_{VL} was not specified. The 4.2 K spectrum clearly contains a weak ferrous component which does not appear in the 80 K spectrum, indicating that at the latter temperature the sixth $3d$ electron of Fe^{2+} has become delocalized. The transition is smeared out vaguely over a broad temperature interval, and specifying a value for T_{VL} is considered to be unwise. Nevertheless, it is beyond any doubt that $Co_{0.4}Fe_{2.6}O_4$ exhibits some kind of electronic transition, be it ill defined, above 4.2 K, thus questioning the result of Rosenberg and Franke,[3] who did not observe any transition for $Co_{0.35}Fe_{2.65}O_4$ down to $T=4.8$ K. The spectra these authors reproduced in their paper clearly show much broader, and hence less structured, absorption lines as compared to those obtained for the present samples. It is therefore conceivable that Rosenberg and Franke missed the minor spectral changes associated with the electronic transition. A poorer homogeneity and/or stoichiometry of their sample is a possible and a reasonable explanation for this lack of spectral details.

As mentioned in paper I of this report, the number of

Mössbauer studies of substituted magnetites $M_xFe_{3-x}O_4$ is quite impressive, especially for composition ranges $x \geq 0.1$, and it is beyond the scope of the present contribution to review, or even make reference to all these papers. A common feature of the spectra is the broad *B*-site line shape which has been explained by the nonunique chemical surrounding of the probe iron nuclei as a result of the unordered distribution of M and Fe ions among the octahedral and/or tetrahedral lattice sites. As a consequence, the *B*-site component has often been described with a discrete, model-dependent hyperfine-field and center-shift distribution consisting of up to six distinct Zeeman patterns. In a few instances, a quasicontinuous, model-independent distribution was applied to fit the *B*-site subpattern.[4,5]

Generally, the involved authors associated the discrete or quasicontinuous range of hyperfine parameters to the existence of different valence states for the iron between and including the pure Fe^{2+} and Fe^{3+} states. However, the derived correlation between the combined hyperfine-field and center-shift values on the one hand, and the valence state on the other hand, and the interpretation of it, is often questionable or contradictory among different research groups. Moreover, in many of those cases considering a discrete model-dependent distribution, either the agreement between the experimental and calculated *B*-site line shape turns out to be rather poor, or the area ratios of the distinct octahedral subspectra as evaluated from the experimental spectra significantly deviate from those expected on the basis of the proposed structural model.

In what follows hereafter, it is demonstrated how a systematic study of the zero-field Mössbauer spectra as a function of temperature and Co substitution, combined with applied-field Mössbauer experiments and using a proper model-independent distribution approach for fitting the spectra, has led to a consistent interpretation of these spectra for compositions $x=0.1$, 0.2, and 0.4, yielding reasonable values for the involved physical quantities in relation to the compositional and structural characteristics of the samples. For $x=0.6$, 0.8, and 0.9, the spectra have become too complicated to retrieve much reliable information from them. Absorbers again consisted of powdered single crystals. The experimental procedures for preparing the absorbers and collecting the spectra were exactly the same as those applied for the low substitutions as described in the first of these two companion papers. A total of more than 150 spectra has been involved in this part of our study. Again, the collection of numerical data is too extensive and will not be reported in detail in this paper. Upon request, all data will be made available.

II. RESULTS AND INTERPRETATION OF THE SPECTRA

A. Curie temperatures

The magnetic order-disorder transition or Curie temperature T_C has been determined for all available compositions by the thermal-scan method with zero source velocity. In all cases, the transition takes place in a relatively sharp temperature interval, which is rather unusual for solid solutions of spinel ferrites. This sharpness is illustrated in Fig. 1 in which the transmission count rate is plotted vs T for the samples with $x=0.6$ and 0.8. The values of T_C, defined as indicated, are plotted against the Co content x in the inset of Fig. 1. For completeness, the data for $x \leq 0.04$ have been included as well. The straight line represents the fitted linear least-squares correlation $T_C=T_C(0)-Cx$, with $T_C(0)=862$ K and $C=55$ K. Extrapolation to $x=1$ leads to $T_C=807$ K, which is in fair agreement with the Curie temperature for slowly cooled $CoFe_2O_4$ (798 K) as found by Sawatzky, van der Woude, and Morrish[6] from Mössbauer experiments. Also, the presently found value $T_C=816$ K for the $x=0.8$ sample is in excellent agreement with that estimated by Fayek and Bahgat for a sample with the same composition, i.e., 814 ± 10 K.[7]

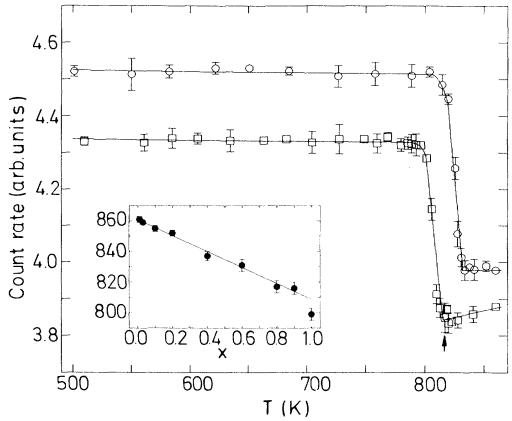

FIG. 1. Thermo-scanning curves at zero source velocity for $Co_{0.6}Fe_{2.4}O_4$ (circles) and $Co_{0.8}Fe_{2.2}O_4$ (squares). Inset: Curie temperature T_C as a function of Co substitution x. Datum for $x=1.0$ is literature value for $CoFe_2O_4$.

Both the sign and the magnitude of the slope of the $T_C(x)$ line are consistent with the weaker *inter*sublattice Co-Fe magnetic exchange interactions as compared to the Fe-Fe interactions. According to Stephenson[8] the Fe_A^{3+}-Co_B^{2+} superexchange integral is about $\frac{1}{16}$th smaller than the Fe_A^{3+}-Fe_B^{2+} superexchange. Moreover, the ferromagnetic double exchange interaction, which results from the electron hopping between the *B*-site irons[9] and which strengthens the antiferromagnetic coupling between *A*- and *B*-site spins, is expected to weaken on increasing the *B*-site substitution.

B. Spectra for $T > T_C$

Above their respective Curie temperatures T_C, the spectra for all the $x \geq 0.1$ samples look similar to those obtained for the compositions described in paper I. Hence, it was at first attempted to interpret these spectra as a superposition of an unsplit *A*-site line and a *B*-site quadrupole doublet. This approach was found to yield straightforward fits for x values of up to 0.4 [see Fig. 2(a),

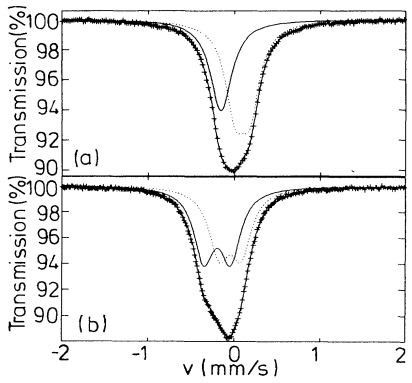

FIG. 2. Mössbauer spectra at 860 K of (a) $Co_{0.2}Fe_{2.8}O_4$ fitted with an A-site singlet and a B-site doublet, and (b) of $Co_{0.9}Fe_{2.1}O_4$ fitted with a superposition of an A- and a B-site quadrupole doublet. The subpatterns plotted in dotted lines refer to the B sites.

$x=0.2$], but failed for $x=0.6$. Models considering, respectively, one A-site singlet and two B-site doublets, one A-site doublet and one B-site doublet, and one A-site doublet and two B-site doublets, all led to divergent iterations or to inconsistent and/or unrealistic values for the various Mössbauer parameters for this composition. On the other hand, acceptable fits for the $x=0.8$ and $x=0.9$ samples were obtained using two quadrupole doublets with equal linewidths, one attributed to B-site iron, the other to A-site iron [see Fig. 2(b), $x=0.9$]. At 860 K the quadrupole splitting $\Delta E_{Q,A}$ of the A-site doublet was found to be 0.28 and 0.31 mm/s, respectively. The A- and B-site center shifts δ_A and δ_B and the B-site quadrupole splitting $\Delta E_{Q,B}$ at 860 K (865 K for $x=0.005$) are plotted as a function of x in Fig. 3. Although the data exhibit some scatter, which should not be surprising considering the strong overlap of the two spectral components, the overall variation with x is clear and significant.

The A-site linewidth at 860 K increases from 0.28 mm/s for $x=0.1$ to 0.35 mm/s for $x=0.4$, and drops again to 0.28 mm/s for $x=0.9$. As for the B sites, Γ_B is constant at 0.28 ± 0.01 mm/s. These results suggest a gradual development of an electric-field gradient (EFG) on the A sites as more and more Co ions are substituted into the lattice. Finally, the relative spectral areas F also depend on x and reflect the gradual removal of iron from the octahedral sites. More quantitative information, however, cannot be drawn from the fitted values for F since these are rather inaccurate as a result of the poor resolution.

C. Spectra for $T < T_C$

In the first stage of this part of the research, the efforts were concentrated on the compositions $x=0.1$, 0.2, and 0.4. Following the suggestions of Franke, Rosenberg and co-workers, who investigated Co-, Ni-, Ge-, Cr-, Al-, and Ga-substituted magnetites at room temperatures (only a very limited number of lower temperatures have been considered by these authors),[3,10–16] the variable-temperature spectra were initially interpreted using one A-site Lorentzian sextet and three or four, depending on x, B-site components. The distinct B sites would originate from different octahedral nearest-neighbor ionic configurations around the probe nuclei. These different configurations were believed to create different average charge states for the B-site irons between 2+ and 3+, and hence different hyperfine fields $H_{\mathrm{hf},B}$ and center shifts δ_B. If all Co ions were randomly distributed in the octahedral sublattice, then the relative spectral areas of the B-site components are given by the binomial probability distribution,

$$P_m=\frac{6!}{m!(6-m)!}\left[\frac{x}{2}\right]^m\left[1-\frac{x}{2}\right]^{6-m}, \tag{1}$$

in which 6 is the total number of B-site nearest neighbors to the central octahedral iron, of which m are Co^{2+}.

In fitting the spectra, the hyperfine parameters H_{hf}, δ and the quadrupole shift ϵ_Q for each sextet were adjustable. All B-site components were assumed to have the

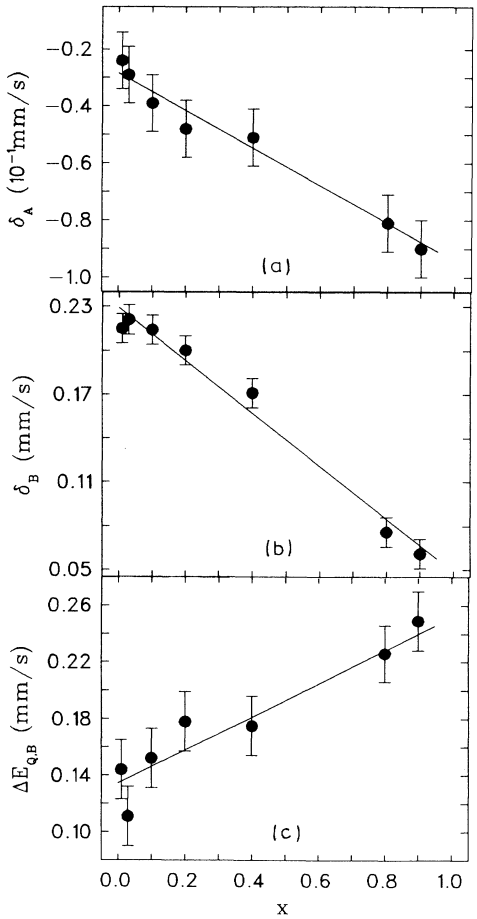

FIG. 3. A-site center shift δ_A, B-site center shift δ_B, and B-site quadrupole splitting $\Delta E_{Q,B}$ plotted vs Co substitution x for $Co_xFe_{3-x}O_4$ at 860 K. The spectrum for $x=0.6$ could not be fitted. The straight lines have no physical meaning.

same two width parameters Γ_B and $\Delta\Gamma_B$ (see paper I), but different from Γ_A and $\Delta\Gamma_A$. The A-site and total B-site absorption areas were adjustable as well, but the relative areas for the different B-site sextets were fixed at their values given by (1). Example fits, referring to $x=0.2$, are shown in Fig. 4. For this composition, the probabilities P_m are calculated as 0.53, 0.35, 0.10, and 0.02 for $m=0$, 1, 2, and 3, respectively. Due to its insignificant contribution, the component corresponding to $m=3$ was not taken into account.

At first glance, the calculated line shapes are in fair agreement with the experimental ones. However, when the temperature variations of the various B-site hyperfine parameters are considered in some detail, one observes a few unacceptable irregularities which seriously question the applied fitting method. The most striking of these is the behavior of the $\delta(T)$ values of the subspectra $B2(m=1)$ and $B3(m=2)$, which initially increase with increasing T up to $T\approx 250$ K and then decrease chaotically on further raising the temperature. Moreover, for $T<500$ K the fitting procedure yields $\delta_{B2}>\delta_{B1}$ and $H_{\mathrm{hf},B2}>H_{\mathrm{hf},B1}$. This finding is inconsistent with the well-established rule saying that a higher center shift points at an ionic character closer to Fe^{2+}, and hence should be associated with a lower hyperfine field. Similar, even more drastic inconsistencies are obvious in the work reported by Franke and Rosenberg,[10] who studied the same solid-solution series ($0.05\leq x\leq 0.7$) at room temperature.

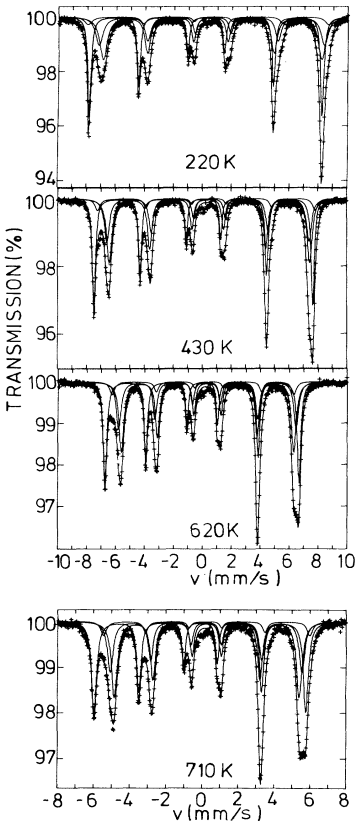

FIG. 4. Mössbauer spectra at a few selected temperatures of $Co_{0.2}Fe_{2.8}O_4$ fitted with a superposition of one A-site subspectrum and three B-site subspectra (full lines).

It should be stressed at this point that allowance for a fraction of the Co ions to enter the A sites will not improve the performance of the above fitting model. As will be discussed below, it is not unlikely that as much as 0.05 Co ions per formula unit are substituting on tetrahedral sites for the composition $x=0.2$. In that extreme case, the probabilities P_m for $x=0.2$ would be 0.63, 0.30, and 0.06 for $m=0$, 1, and 2, respectively. Fixing the relative areas of the B-site components to these values will not significantly alter the goodness of fit χ^2, nor the derived hyperfine parameters.

The observed inconsistencies raise one's suspicion that the model based on a limited number of B-site components, associated with the random distribution of Co in the nearest-neighbor B-site cation shell of the probe nuclei, is a too crude approximation for the real situation, in which chemical-disorder effects extending over a range beyond nearest neighbors are not unimportant. Therefore, all presently obtained spectra have been described by a superposition of an A- and a B-site model-independent hyperfine-field distribution, the latter one with linear correlations between the center shift and the hyperfine field, and between the quadrupole shift and the hyperfine field.[17] Depending on T, 6–10 different field values for the A-site component, and 15–25 for the B-site component were considered, increments of 3 and 5 kOe, respectively. Several fits were carried out for any given T and x in order to determine the upper and lower limits of the two H_{hf} intervals yielding the lowest χ^2. The elementary A- and B-site linewidths were adjusted independently from one another and were generally broader for the B-site component (e.g., $\Gamma_A=0.23$ mm/s and $\Gamma_B=0.29$ mms/s for $x=0.2$ at $T=300$ K). Typically, the χ^2 arrived at by this model-independent approach was 25% lower as compared to the value for the fitting model based on expression (1).

Selected H_{hf}-distribution profiles $p(H_{\mathrm{hf}})$, referring to $Co_{0.2}Fe_{2.8}O_4$, are reproduced in Fig. 5. The A-site distribution is narrow and almost perfectly symmetric. The bimodal structure of the B-site profile $p(H_{\mathrm{hf},B})$ has been found for all T values below ≈ 650 K, and moreover for $x=0.1$ and $x=0.4$ as well. This finding implies the existence of two clearly distinct Fe_B states—further denoted by $B1$ (highest fields) and $B0$–for the intermediate compositions $0.1\leq x\leq 0.4$ at temperatures below ≈ 650 K. The Mössbauer parameters for each of these two B states are distributed as a result of fluctuating structural and electronic environments. At higher temperatures, the $B1$ state gradually disappears and the smoothness of the temperature variation of the $B0$ hyperfine parameters suggest that it transforms into $B0$.

The maximum-probability hyperfine fields $H^m_{\mathrm{hf},i}(i=A,B1,B0)$, the center shifts δ_A or δ^m_{Bi} (the superscript m refers to the values corresponding to $H^m_{\mathrm{hf},i}$), and the relative spectral areas F_i are listed in Table I for the $x=0.2$ sample at selected temperatures. These figures were obtained from adjusting Gaussian functions to the evaluated histograms (full lines in Fig. 5). The er-

rors are, respectively, 2 kOe, 0.01 mm/s, and 2% for the A-site distribution, and at least twice as much for the B-site ones. Although the $B1$ parameters seem to vary consistently with T, their values are to be considered unreliable, especially those for δ^m_{B1}. Table II contains the same data for the three samples at two different temperatures, i.e., $T=180$ and 250 K. All results for the tetrahedral ferric ions are perfectly in line with those obtained from the aforementioned model-dependent fitting approach. The coefficient of the linear $H_{\mathrm{hf},B}$-δ_B correlation for a given x was found to be fairly constant throughout the entire temperature range. The average values are -0.0013, -0.0016, and -0.0025 mm/s kOe for $x=0.1$, 0.2, and 0.4, respectively. In all cases, the A-site and $B0$-state quadrupole shifts were found to be zero within experimental error limits. In contrast, the $B1$ quadrupole shifts are nonzero and negative, and their magnitude decreases with increasing T and, at a given T, with increasing x. Since no additional information could be retrieved from the various quadrupole-shift parameters, their iterated values are not included in Tables I and II.

For Co substitutions $x \geq 0.6$, for which only two selected temperatures were considered (180 and 250 K), the fitting results no longer support the existence of two distinct B states with clearly resolved hyperfine-field distributions. Figures 6(a) and 6(b) show the spectra recorded for $Co_{0.6}Fe_{2.4}O_4$ and $Co_{0.9}Fe_{2.1}O_4$ at 180 K. The full lines are again the result of fitting two model-independent H_{hf} distributions and the evaluated distribution profiles are depicted in Figs. 6(c) and 6(d), respectively. The A-site distributions remain quite narrow, but the B-site ones no longer exhibit two well-separated maxima as in the case of lower Co substitutions. Instead the presence of at least three or four major B-site components, each having a broad range of hyperfine parameters, seems to be implied by the calculated profiles. The quantitative characteristics of these components are, however, poorly defined, except those for the highest-field component. For this latter one, the Mössbauer parameters for the three involved compositions were observed to vary with x in a manner that complements the observed variation with x of the $B1$ parameters for the intermediate substitutions (see Table II). Therefore, this high-field component is assigned to a configuration similar to the configuration which gives rise to the $B1$ component in the spectra of the samples with $x=0.1$, 0.2, and 0.4.

Spectra in longitudinal external fields of $H_{\mathrm{ext}}=55$ kOe were collected for the samples with $x=0.1$, 0.2, and 0.4 at 180 and 250 K in an attempt to confirm the bimodal structure of $p(H_{\mathrm{hf},B})$. The spectra for $x=0.2$ and 0.4 at 250 K are shown in Fig. 7(a). From these, the existence of two distinct B sites is clearly evidenced. The spectra were again described by a superposition of one A-site and

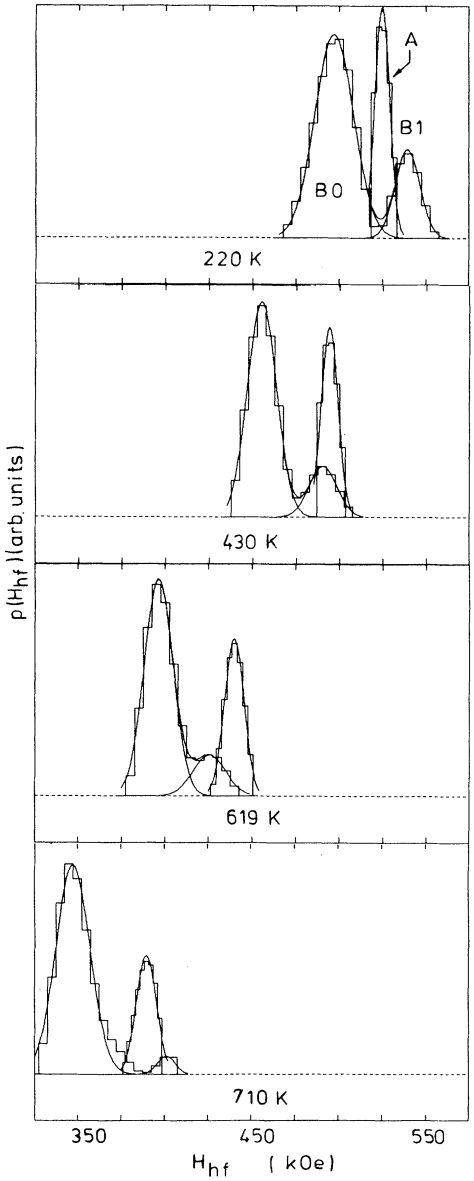

FIG. 5. Hyperfine-field distributions $p(H_{\mathrm{hf}})$ evaluated from the spectra of Fig. 4, clearly showing the presence of two distinct B sites. The solid lines are the Gaussian curves and their superposition fitted to the $p(H_{\mathrm{hf}})$ histograms.

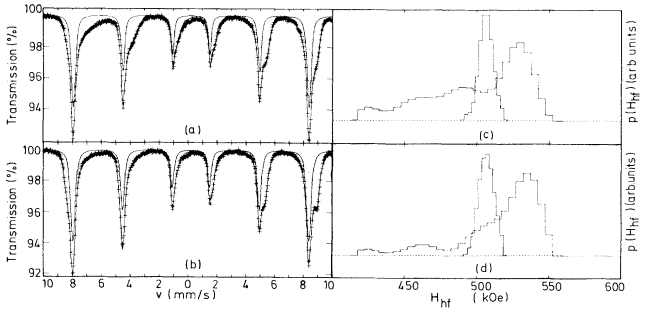

FIG. 6. Mössbauer spectra at 180 K of (a) $Co_{0.6}Fe_{2.4}O_4$ and (b) $Co_{0.9}Fe_{2.1}O_4$. The distributed B-site components are plotted in dotted lines. The derived hyperfine-field distributions are shown in (c) and (d), respectively.

TABLE I. Relevant Mössbauer parameters derived from the model-independent hyperfine-field distributions fitted to the spectra of $Co_{0.2}Fe_{2.8}O_4$ at selected temperatures. $B1$ and $B0$ refer to the two maxima in the distribution profiles of the B-site component. Center shifts δ are with respect to metallic iron at room temperature.

T (K)	A sites			$B1$ sites			$B0$ sites		
	$H^m_{hf,A}$ (kOe)	δ_A (mm/s)	F_A (%)	$H^m_{hf,B1}$ (kOe)	δ^m_{B1} (mm/s)	F_{B1} (%)	$H^m_{hf,B0}$ (kOe)	δ^m_{B0} (mm/s)	F_{B0} (%)
120	506	0.35	40	531	0.69	12	492	0.76	48
200	502	0.31	39	518	0.65	14	476	0.71	48
300	492	0.27	39	500	0.59	12	459	0.64	50
390	479	0.21	39	478	0.54	11	441	0.58	50
494	454	0.15	39	446	0.47	12	413	0.51	50
590	425	0.08	38	413	0.41	12	381	0.45	51
710	366	0.01	37	352	0.35	9	321	0.36	54
770	308	−0.02	39	290	0.28	7	270	0.30	54

one B-site hyperfine-field distribution [Fig. 7(b)], the latter with linear H_{hfB}-δ_B correlation. The resolution of the distinct spectral components has dramatically improved as compared to the zero-field spectra, and hence it is conceivable that the retrieved quantitative results (Table III), in particular the relative areas of the different components, are more accurate and reliable, although the F_{B1} and F_{B0} values are surprisingly close to those evaluated from the zero-field spectra. The center shifts of Fe_{B1}, however, differ markedly from the values listed in Table II.

The maximum-probability hyperfine fields $H^m_{hf,i}$ ($i = A, B1, B0$) indicated in Table III were deduced from the corresponding effective fields $H^m_{eff,i}$ assuming that H_{ext} fully adds to the A-site hyperfine fields, and fully subtracts from the B-site ones. Due to the relatively large errors on the various hyperfine-field parameters (compared to the data for $x \leq 0.04$), it is not possible to conclude whether that assumption is correct for all three components, and small deviations such as those observed for the B-site fields in the samples with $x \leq 0.04$ (Fig. 10 in paper I) are not expected to be obvious for the higher substitutions. In general, there appears to be a reasonably good agreement between the $H^m_{hf,i}$ values of Table III and those from the zero-field spectra, except perhaps for the $B0$ component for which the addition

TABLE II. Relevant Mössbauer parameters derived from the model-independent hyperfine-field distributions fitted to the spectra of $Co_xFe_{3-x}O_4$ at 180 K (upper half) and 250 K (lower half). For $x = 0.6$, 0.8, and 0.9 more than two B-site components are present and only the one with the highest maximum-probability field can be quantified with reasonable precision. The results for $x = 1$ are extrapolated values and values obtained from the spectra of $CoFe_2O_4$.

x	A sites			$B1$ sites			$B0$ sites		
	$H^m_{hf,A}$ (kOe)	δ_A (mm/s)	F_A (%)	$H^m_{hf,B1}$ (kOe)	δ^m_{B1} (mm/s)	F_{B1} (%)	$H^m_{hf,B0}$ (kOe)	δ^m_{B0} (mm/s)	F_{B0} (%)
0.1	502	0.32	36	518	0.68	7	477	0.73	57
0.2	503	0.32	39	520	0.66	14	481	0.73	48
0.4	504	0.32	40	525	0.60	23	482	0.71	37
0.6	506	0.32	40	529	0.51				
0.8	507	0.32	45	534	0.49				
0.9	507	0.32	46	535	0.47				
1.0[a]	508	0.32		537	0.44				
1.0[b]	506	0.28	46	541	0.43				
0.1	497	0.29	37	508	0.64	7	467	0.68	57
0.2	497	0.29	38	510	0.61	13	469	0.67	50
0.4	498	0.29	39	512	0.57	26	470	0.67	35
0.6	500	0.29	43	519	0.51				
0.8	500	0.28	61	526	0.48				
0.9	500	0.28	63	526	0.46				
1.0[a]	501	0.28		530	0.43				
1.0[b]	496	0.24	46	528	0.38				

[a]Extrapolated values.
[b]Values for $CoFe_2O_4$.

TABLE III. Relevant Mössbauer parameters derived from the model-independent hyperfine-field distributions fitted to the spectra of $Co_xFe_{3-x}O_4$ ($x=0.1$, 0.2, and 0.4) at 180 K (upper half) and 250 K (lower half) in a longitudinal external magnetic field of $H_{ext}=55$ kOe. The maximum-probability hyperfine fields $H^m_{hf,i}$ ($i=A,B1,B0$) were obtained from the corresponding effective fields $H^m_{eff,i}$ assuming that H_{ext} fully adds to the A-site hyperfine fields, and fully subtracts from the B-site hyperfine fields.

	A sites			$B1$ sites			$B0$ sites		
x	$H^m_{hf,A}$ (kOe)	δ_A (mm/s)	F_A (%)	$H^m_{hf,B1}$ (kOe)	δ^m_{B1} (mm/s)	F_{B1} (%)	$H^m_{hf,B0}$ (kOe)	δ^m_{B0} (mm/s)	F_{B0} (%)
0.1	501	0.32	34	521	0.60	9	481	0.74	57
0.2	500	0.32	34	520	0.57	16	480	0.73	50
0.4	502	0.31	35	523	0.51	25	486	0.72	40
0.1	496	0.29	35	508	0.60	9	471	0.69	57
0.2	495	0.28	35	509	0.56	17	471	0.69	49
0.4	497	0.28	35	515	0.51	24	474	0.67	41

$H^m_{eff,B0}+H_{ext}$ shows the tendency to exceed the corresponding zero-field $H^m_{hf,B0}$ value by about 4 kOe.

A final note concerns the $\Delta m_I=0$ transition lines (middle lines in Fig. 1) which have not completely vanished in the external-field spectra (Fig. 7), their intensity slightly increasing with increasing Co content. This effect is due to the high magnetic anisotropy of octahedral Co^{2+} ions, implying that strong magnetic fields are required to align the spin structure along the direction of the field. This feature is very obvious for $CoFe_2O_4$, for which at 4.2 K in a field of 60 kOe the spins make an angle of $\approx 28°$ with respect to the field direction.[18] For the present sample with $x=0.4$, the angle is only a few degrees and does therefore not affect the validity of the listed hyperfine-field values.

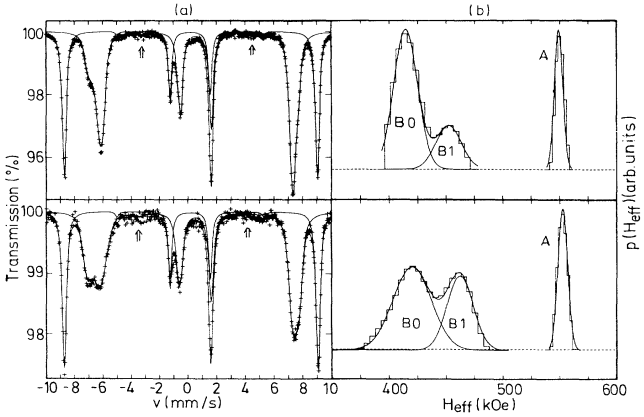

FIG. 7. (a) Mössbauer spectra recorded at 250 K in an applied longitudinal magnetic field of 55 kOe; top: $x=0.2$; bottom: $x=0.4$. The solid lines are the distributed A- and B-site components and their sum, adjusted to the experimental data. Note the presence of the $\Delta m_I=0$ lines (arrows), which were taken into account in fitting the spectra. The evaluated distribution profiles $p(H_{hf})$ are shown in (b). The solid lines in (b) are the Gaussian curves fitted to the $p(H_{hf})$ histograms.

III. DISCUSSION

A. Cation distribution

The distribution of Fe among the octahedral and tetrahedral lattice sites can be estimated from the evaluated relative spectral areas F_A, for which reliable values were obtained for the $x=0.1$, 0.2, and 0.4 samples only from the external-field measurements (Table III). Taking into account the slightly different Mössbauer fractions f for tetrahedral and octahedral iron as calculated from the corresponding characteristic Mössbauer temperatures Θ_M (Sec. III C), the number of Co ions on A sites per formula unit is estimated to be ≈ 0.0, 0.05, and 0.1, respectively.

The F_A values obtained from the zero-field spectra of the samples with $x \geq 0.6$ are less accurate. The results in that respect for $x=0.8$ and 0.9 at 250 K are unrealistic, while those at 180 K would indicate an inversion degree of ≈ 0.9 for both samples. This datum seems reasonable, considering the inversion degree of a slowly cooled sample of $CoFe_2O_4$ as obtained from the external-field (60 kOe) spectrum at 4.2 K, i.e., 0.9 as well.[18]

B. Origin of the distinct B-site components

The maximum-probability hyperfine fields $H^m_{hf,Bi}$, and center shifts δ^m_{Bi} of the two distributed B-site components at 180 and 250 K are plotted against the Co content x in Fig. 8. Both quantities vary with x in a more or less linear fashion and the full lines in the drawings represent the linear least-squares fits. The $B1$ values obtained from extrapolation to $x=1$, are indicated in Table II as well. For comparison, the A- and B-site Mössbauer parameters for a polycrystalline $CoFe_2O_4$ sample, with 10% of the Co ions on the A sites,[18] are also included. They were derived from the spectra by fitting a superposition of an A-site sextet and a B-site, model-independent H_{hf} distribution. The results suggest that the $B1$ component in $Co_{0.1}Fe_{2.9}O_4$ arises from iron which has a nominal charge somewhere between 2.5+ and 3+, and, on further increasing the Co substitution, gradually evolves towards the pure Fe^{3+} state of $CoFe_2O_4$.

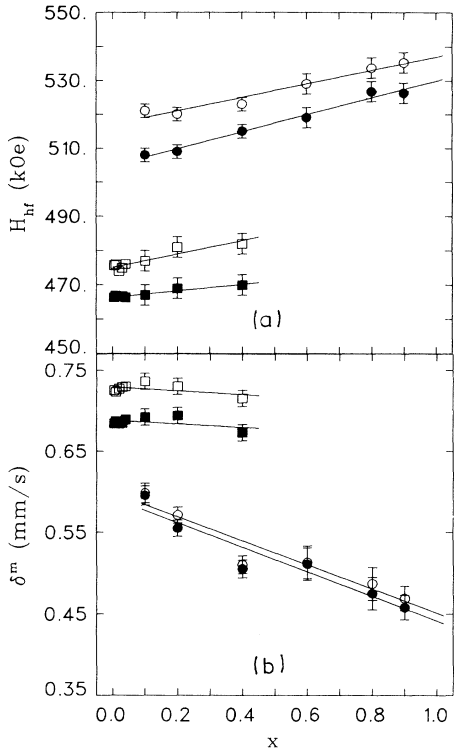

FIG. 8. Maximum-probability hyperfine fields (a) and center shifts (b) of the two B-site components, $B1$ (circles) and $B0$ (squares), resolved from the Mössbauer spectra of $Co_xFe_{3-x}O_4$ at 180 K (open symbols) and 250 K (filled symbols). Solid lines are linear least-squares fits.

The $B0$ parameters in Fig. 8, in particular the center shifts, exhibit a weaker variation with x as compared to the $B1$ ones and are nicely in line with the data for the $x \leq 0.04$ compositions. This finding suggests that the $B0$ component is caused by Fe ions which are involved in an electron-exchange process similar to that taking place in the non- or poorly substituted magnetites. The observations that the $B0$ hyperfine field as determined from the external-field spectra is somewhat higher than its value derived from the zero-field spectra, is consistent with that suggestion, since a similar effect was observed for the B-site hyperfine field in the samples with $x \leq 0.04$.

It is conceivable to attribute the existence of two B-site components (for T smaller than ≈ 650 K) to the presence of a substantial amount of Co in the octahedral sublattice. A perspective view of this sublattice is represented in Fig. 9, showing that the octahedral sites form tetrahedra which are linked to one another by sharing vertices. According to Anderson's criterion for inverse ferrites,[19] each tetrahedron contains two bivalent and two trivalent cations. In order to determine the possible configurations which originate from substituting Co^{2+} in Fe_3O_4, one can therefore confine his attention to a single tetrahedron. Suppose site 1 in Fig. 9 is occupied by the probe iron nucleus. Then, of the remaining sites 2, 3, and 4, a maximum of two can host a Co ion, and hence only three configurations for the involved tetrahedron are possible,

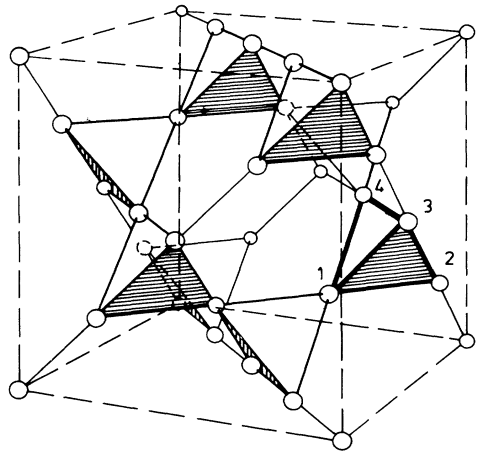

FIG. 9. Octahedral sublattice of a spinel structure.

i.e., zero, one, or two vertices consisting of Co. The respective probabilities P_0, P_1, and P_2 are easily calculated from a binomial law, similar to (1), but with three instead of six possible sites for the Co ions. They are listed in Table IV for the relevant x values up to 0.6, in which the fraction of A-site Co was taken into account (this fraction for $x=0.6$ was taken equal to that of $x=0.4$). The spectral areas of $B1$ and $B0$, relative to the total B-site area, are indicated as well.

On the basis of the data presented in Table IV, one is inclined to attribute the $B0$ component to iron nuclei for which at least one of the two B-site tetrahedra to which they belong does not contain any Co, and the $B1$ component to all other iron nuclei. If this picture is correct, then a major question remains to be answered, i.e., whether it is consistent with the observed $B1$ and $B0$ parameters displayed in Fig. 8.

If a particular B-site tetrahedron is exclusively occupied by Fe, the two nonlocalized $3d$ electrons are shared by four irons, leading to an average charge state of 2.5+, as in nonsubstituted Fe_3O_4. This valence state in magnetite yields at 250 K a B-site field of 465 kOe and a center shift of 0.69 mm/s (see paper I), both values being reasonably close to those for the $B0$ component of the $x=0.1$ sample (see Table II). If, on the other hand, one of the four vertices is occupied by Co, then one electron is shared by three irons, leading to an average charge

TABLE IV. Probabilities P_i of having i Co ions in the B-site tetrahedron containing the probe iron nucleus, and relative spectral areas of $B0$ and $B1$ components in the external-field Mössbauer spectra.

x	P_0	P_1	P_2	$F_{B0}/(F_{B1}+F_{B0})$	$F_{B1}/(F_{B1}+F_{B0})$
0.1	0.857	0.135	0.006	0.86	0.14
0.2	0.791	0.193	0.016	0.76	0.24
0.4	0.614	0.325	0.057	0.62	0.38
0.6	0.422	0.422	0.141		

state of 2.7+. Assuming to a first approximation that the hyperfine field of octahedral iron is proportional to its average number $\langle n_{3d} \rangle$ of $3d$ electrons (orbital and dipolar fields are extremely small—see paper I), this 2.7+ charge would correspond to a hyperfine field of 502 kOe, which is close to the value obtained by extrapolating the $H^m_{\mathrm{hf},B1}(x)$ line [filled circles in Fig. 8(a)] to $x=0.0$, i.e., 505 kOe.

Furthermore, a change $\Delta\langle n_{3d} \rangle$ causes a change in the center shift which is, again to a good approximation, proportional to $\Delta\langle n_{3d} \rangle$.[20] A very typical δ value for octahedral Fe^{3+} in spinel ferrites at 250 K is 0.38 mm/s, which is also the value found for $CoFe_2O_4$ (see Table II). Knowing that the 2.5+ charge in Fe_3O_4 corresponds to $\delta=0.69$ mm/s (250 K), it is easily calculated that a 2.7+ charge should yield $\delta=0.57$ mm/s. Extrapolating the $\delta^m_{B1}(x)$ line [filled circles in Fig. 8(b)] to $x=0.0$ yields $\delta^m_{B1}(0)=0.59$ mm/s, in good agreement with the above derived value.

In summary, both the parameter values for δ and H_{hf}, and the relative spectral areas of $B1$ and $B0$ are consistent with the proposed explanation, based on the distribution of Co among the B-site tetrahedra, for the existence of two distinct octahedral irons for Co substitutions of up to $x=0.4$. The fact that these two iron sites have nonunique hyperfine interactions can qualitatively be attributed to second-order effects caused by the Co ions on nearest-neighbor A sites and next-nearest-neighbor B sites. The observation that both distributions broaden with increasing x corroborates this suggestion.

At temperatures exceeding $\approx$650 K, the $B1$ component gradually disappears in favor of the $B0$ component. This feature can be explained assuming that, as a result of thermal activation, the electron-exchange process, which takes place between the $B0$ sites at lower temperatures, involves all iron ions at high temperatures. It could be that the high mobility of the Co ions triggers the "expansion" of that exchange process. The relative variation of the lattice constant of $CoFe_2O_4$ as a function of the quenching temperature,[21] indeed clearly shows that ionic migration starts at about 400 °C. It should be mentioned at this point that the appearance of one single B-site component in the magnetic spectra at high temperatures is strongly supported by the results derived from the paramagnetic spectra (see Sec. II D).

For $x \geq 0.6$, the electronic structure, and hence the magnetic one as well, is more complicated and only a few qualitative conclusions can be drawn from the results obtained from the data analyses. The shape of the evaluated $p(H_{\mathrm{hf},B})$ profiles suggests that more than two valence states are present. It is no problem to adjust a sum of four Gaussian distributions to the $p(H_{\mathrm{hf},B})$ histograms reproduced in Figs. 6(c) and 6(d). For $x=0.9$ at 180 K this procedure yields hyperfine fields and spectral areas relative to the total B-site area of, respectively, 536 kOe and 0.47, 513 and 0.41, 462 and 0.09, and 425 and 0.03. The latter one, with corresponding center shift $\delta=0.75$ mm/s, possibly results from Fe^{2+} ions with localized $3d$ electrons, although the δ value, despite being very inaccurate, is rather low. The 462-kOe component, with $\delta=0.65$ mm/s, indicates that some of the irons are still involved in an electron-exchange process. Finally, the two major components, further denoted $B1_0$ (highest field) and $B1_1$, can be attributed to Fe^{3+} and a tentative explanation of their origin is discussed next.

Due to the presence of a fraction x_A of Co ions in the tetrahedral sublattice, the B-site irons experience a nonunique nearest-neighbor A-site configuration, and hence a discrete number of different hyperfine fields as a consequence of the well-known A-to-B supertransfer mechanism. The probability P_m that a probe B-site nucleus has $m\,Co^{2+}$ and $(6\text{-}m)Fe^{3+}$ cations for nearest A-site neighbors is given by expression (1) in which $x/2$ is replaced by x_A. This yields $P_m=0.53$, 0.35, 0.10, and 0.02 for $m=0$, 1, 2, and 3, respectively, hereby assuming $x_A=0.10$. If the above mentioned value of 536 kOe for $B1_0$ is considered as the B-site hyperfine field corresponding to an A-site configuration with six Fe^{3+} ions, and assuming that the supertransferred hyperfine field for the involved sample is equal to that for $CoFe_2O_4$, i.e., 18 kOe at 180 K,[18] then the configurations $m=1$, 2, and 3 lead to field values of 518, 500, and 482 kOe, respectively. It is not unreasonable to assume further that these three latter components are not resolved by the distribution fits, but instead superimpose to one broad distribution centered around the weighed average of the three field values, which is 513 kOe, in excellent agreement with the maximum-probability field of $B1_1$. It is important to note at this point that the spread of the $B1_1$ Gaussian distribution is calculated to be approximately twice the value for the $B1_0$ distribution. Finally, if P_0 and the summation $(P_1+P_2+P_3)$ are normalized with respect to the total area of the adjusted $B1_0$ and $B1_1$ distributions, i.e, 0.88, one finds the value 0.47 and 0.41, respectively, which is again in excellent agreement with the adjusted values.

In summary, the suggestion that $B1_0$ is attributable to B-site Fe^{3+} with no Co ions in its nearest-neighbor A-site shell, and $B1_1$ to all other B-site Fe^{3+}, is strongly supported by the numerical results derived from the $p(H_{\mathrm{hf},B})$ data. Similar consistent results were found for the $x=0.8$ and $x=0.6$ samples, with a somewhat poorer, but still reasonable agreement between the parameters obtained from adjusting four Gaussian distributions, and the values one would expect on the basis of the proposed structural model.

As a justified criticism against the above reasoning, one could argue that the broad component representing the combined $m=1$, 2, and 3 configurations has been described by a symmetric distribution, which is obviously not the case. It was initially believed that such an approximation would not drastically affect the relevant distribution parameters in the sense that they would no longer be consistent with the structural model. In order to be reassured about that belief, a fifth Gaussian distribution was introduced in fitting the $p(H_{\mathrm{hf},B})$ data for $x=0.9$ at 180 K. The idea behind this attempt was to take into account different components $B1_0$, $B1_1$, and $B1_2$, corresponding to the A-site configurations with $m=0$, 1, and 2, respectively (the $m=3$ component has been omitted due to its insignificant contribution). How-

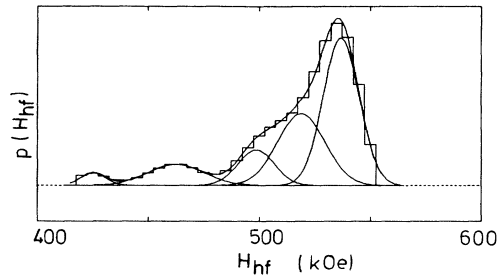

FIG. 10. B-site hyperfine-field distribution $p(H_{\mathrm{hf},B})$ of $Co_{0.9}Fe_{2.1}O_4$ at 180 K fitted with a superposition of five Gaussian distributions.

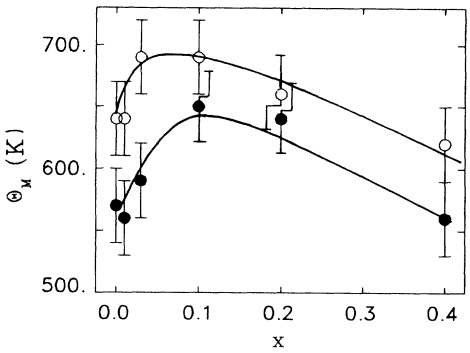

FIG. 11. Characteristic Mössbauer temperatures Θ_M as a function of x for $Co_xFe_{3-x}O_4$. Open circles represent A sites, filled circles B sites ($x=0,0.01,0.03$) or $B0$ states ($x=0.1,0.2,0.4$). Solid curves serve as a guide for the eye.

ever, without any restriction with respect to the adjustable parameters of all five distributions, the fit could not reach convergency with reasonable parameter values. Therefore, it was imposed that the central field of the $B1_1$ distribution should be 18 kOe less than the $B1_0$ field. With this one and only restriction a very good reproduction of the $p(H_{\mathrm{hf},B})$ data was finally obtained (see Fig. 10).

The parameters for the two weak low-field distributions are not affected by the introduction of the fifth Gaussian distribution. The central fields of the other three components were iterated to be 537, 519, and 499 kOe for $B1_0$, $B1_1$, and $B1_2$, respectively, and their relative contributions, normalized to one, are 0.53, 0.34, and 0.13. All these figures are in remarkable agreement with the ones predicted by the structural model proposed to explain the appearance of the different $B1_i$ components. They further prove that from numerical point of view the $B1_1$ and $B1_2$ distributions can be represented by one single Gaussian distribution without obscuring the physical characteristics which are reflected in the $p(H_{\mathrm{hf},B})$ profiles and which can be deduced from these profiles by careful analysis.

C. Temperature variation of the hyperfine parameters

As mentioned earlier in this paper, the values of the $B1$ Mössbauer parameters obtained from the zero-field spectra for $x=0.1$, 0.2, and 0.4 are rather inaccurate due to the strong overlap of these components with the A-site subpatterns. The temperature variation of these parameters has therefore received little further attention.

The temperature dependence of the A- and $B0$-site center shifts δ were interpreted in the same manner as described and applied in paper I of this study. The obtained intrinsic isomer shifts δ_I, i.e., 0.56 ± 0.01 mm/s for A and 0.98 ± 0.01 mm/s for $B0$, do not differ significantly from the values found for the samples with $x\leq0.04$. The characteristic Mössbauer temperatures, including those for $x=0.0$, 0.01, and 0.03 are plotted against x in Fig. 11. Both $\Theta_{M,A}$ and $\Theta_{M,B0}$ seem to show a maximum at x around 0.1. However, considering the poor sensitivity of the shape of the calculated $\delta(T)$ curve to the iterated parameter values, it is not beyond any doubt that this feature is real. If it is, the authors could not think of any reasonable explanation for this maximum.

It should be mentioned at this point that the unusual behavior of $\delta_A(T)$ for T exceeding ≈700 K, as observed for the $x\leq0.04$ samples, does occur for the higher substitutions as well, though to a lesser extent. This would mean that high Co contents oppose the A-site irons to get involved in the electron-exchange process at high temperatures. This finding does not sound unreasonable in spite of the conclusion arrived at in paper I that the presence of a small amount of Co in the octahedral sublattice initially enhances the involvement for some unknown reason.

The fact that $\Theta_{M,A}$ is larger than $\Theta_{M,B0}$ implies that the radio f_A/f_{B0} (or f_A/f_B for small x) of the A- and $B0$- (or B-) site Mössbauer fractions calculated from $\Theta_{M,A}$ and $\Theta_{M,B0}$ (Ref. 49, paper I), is larger than unity at any given temperature. The deviation, however, is calculated to be small: at 180 K and room temperature (RT), the ratio does not exceed 1.03 and 1.04, respectively. Sawatzky, van der Woude, and Morrish[22] found for Fe_3O_4 at RT $f_A/f_B=1.06\pm0.02$ from the temperature dependence of the relative areas F_A and F_B of the A- and B-site subspectra. Their method applied to the results of samples $x=0.01$ and $x=0.03$ (the F_A/F_{B0} data for higher substitutions are too inaccurate) has yielded $f_A/f_B=1.08\pm0.03$ at RT in both cases, and is in good agreement with the previous value.

The reduced A-site hyperfine fields when plotted vs the reduced temperature follow a curve which is visually identical for the three involved intermediate compositions, and which moreover coincides with the curve obtained for any of the samples with $x\leq0.04$. As expected for this reason, the experimental $H_{\mathrm{hf},A}(T)$ variations are again very well described by a Brillouin function, approximating the reduced B-site sublattice magnetization at any given T, which appears in the expression for the A-site molecular field, by the experimentally observed value for the reduced hyperfine field of the dominant $B0$ component. The adjusted values of the A-A and A-B superexchange integrals J_{AA} and J_{AB} vary in the range

10.5±0.5 K and 21.5±1.0 K, respectively, and evidence that J_{AB} would decrease with increasing x is not reflected in the obtained results. The observed $H_{\mathrm{hf},A}(T)$ data are reproduced to within 0.5%, except for the highest temperatures in the vicinity of T_C, for which deviations of 3% are not uncommon. It is not impossible that the involvement of the A-site irons in the electron-exchange process contributes to these enhanced deviations. On the other hand, one should bear in mind that at temperatures near T_C, the collapsing of the magnetic spectra causes a much stronger overlap between A- and B-site subpatterns and hence more poorly defined Mössbauer parameters.

It was attempted to fit the non-localized-electron model (NLEM), the basic expressions of which are indicated in paper I, to the temperature variation of the $H_{\mathrm{hf},B0}$ data. Although the adjusted values for the involved physical quantities seem to be reasonable, the experimentally observed $H_{\mathrm{hf},B0}(T)$ curve is not adequately reproduced by the calculated one, the deviations becoming larger with increasing x. This, however, should not be surprising since the NLEM is applicable only for an unperturbed electron-exchange process between ions on equivalent lattice sites. This condition is certainly not fulfilled for the present samples, for which the substantial Co substitution creates a complicated electronic structure for the B-site iron species. It is believed that a more adequate physical model to describe $H_{\mathrm{hf},B0}(T)$ cannot be conceived.

D. Paramagnetic spectra

The sharp linewidth of the B-site quadrupole doublet for the samples with $x=0.1$, 0.2, and 0.4 at $T>T_C$, i.e., $\Gamma_B \approx 0.28$ mm/s at 860 K, which is also the value of Γ_B for $x \leq 0.04$, confirms the existence of only one single B-site iron state at high temperatures. If, indeed, the $B0$ and $B1$ components would both be present, one would expect a much broader linewidth, especially for $x=0.4$ for which the two B-site subpatterns have comparable line areas and center shifts which differ by ≈ 0.1 mm/s (see Table III).

From the variation with x of both A- and B-site center shifts (see Fig. 3), one can conclude that the involvement of Fe_A^{3+} in the electron-exchange process gradually diminishes with increasing Co substitution and that simultaneously the electronic state of Fe_B more and more approaches 3+. Further, the presence of Co^{2+} ions in the lattice creates a less symmetrical charge distribution around the probe iron nuclei and this explains the increasing quadrupole interactions with increasing x.

IV. SUMMARY AND CONCLUSION

It has been demonstrated that the variable-temperature Mössbauer spectra of Co-substituted magnetites $Co_xFe_{3-x}O_4$ with $x \geq 0.1$ are adequately and consistently described by a superposition of two model-independent hyperfine-field distributions, one arising from the tetrahedral (A) iron species, the second one from the octahedral (B) irons. It was found necessary to introduce a linear correlation between the hyperfine field and the center shift for the distributed B-site component in order to obtain reasonable goodness-of-fit values. In the composition range $x=0.1-x=0.4$, the evaluated distributions reflect the existence of two distinct electronic states for the B-site irons at temperatures not exceeding ≈ 650 K. This feature is irrefutably confirmed by the external-field spectra recorded at two different temperatures. The B-site component ($B0$) with the weaker hyperfine fields and higher center shifts is due to iron species which are involved in an electron-exchange process similar to that occurring in the samples with a Co content $x \leq 0.04$. It is attributed to nuclei which have no Co nearest neighbor in at least one of the two B-site tetrahedra to which each nucleus belongs. The other possible configurations are suggested to give rise to the second component ($B1$), the hyperfine-interaction data of which point at a time-averaged valence state between 2.5+ and 3+, which gradually shifts towards the latter as x increases.

At high temperatures, the $B1$ component in the magnetic spectra gradually disappears in favor of $B0$, indicating that all B-site irons are involved in one single electron-exchange process. The paramagnetic spectra have confirmed this finding.

The temperature variation of the center shifts has been interpreted in terms of a temperature-dependent intrinsic isomer shift δ_I, combined with the Debye model for the second-order Doppler shift. The behavior of the A-site center shifts at high temperature is similar to that observed for the samples with $x \leq 0.04$, suggesting that at these high temperatures the A sites become involved in the electron-exchange process. The 0-K δ_I values of the A- and $B0$-site irons in the range $0.0 \leq x \leq 0.4$ do not vary significantly with x. The characteristic Mössbauer temperatures seem to exhibit a maximum value for x around 0.1.

The A-site hyperfine field is adequately described by a Brillouin function (localized-electron model), in which the reduced B-site sublattice magnetization is taken equal to the reduced B-site hyperfine field. The obtained values for the A-A and A-B superexchange integrals give no indication as to whether they depend on the Co concentration. The non-localized-electron model, which was successfully applied to describe the temperature dependence of the octahedral hyperfine field for the $x \leq 0.04$ samples, was unsuccessful for the higher substitutions. As for the $B1$ component, its Mössbauer parameters are considered to be too inaccurate and unreliable to enable any meaningful conclusions to be retrieved from their temperature behavior.

In contrast to the A-site distribution, which remains sharp and quite symmetric, the shape of the B-site hyperfine-field distribution for the substitutions $x=0.6$, 0.8, and 0.9 is much more complicated and indicates the presence of several average charge states for the iron species. It is believed that due to that complexity, a detailed study of the temperature dependence of the spectra will not produce valuable and reliable conclusions with respect to the magnetic and electronic properties of these ferrites in relation to their structure and composition. As could be proven, an additional complication appears as a result of the random distribution of Co and Fe cations on

the tetrahedral sublattice. This randomness has for consequence that each B-site spectral component is asymmetrically broadened due to fluctuations in the nearest-neighbor A-site configuration of the octahedral Mössbauer nuclei.

Notwithstanding this chemical disorder, the magnetic order-disorder transition remains sharp for all compositions. The Curie temperature slightly decreases with increasing Co content. The paramagnetic spectra for $x=0.1$, 0.2, and 0.4 could be decomposed into an A-site singlet and a B-site doublet. For higher substitutions the disordered cationic charge distribution creates an electric-field gradient on the tetrahedral sites as well. The isomer shifts decrease with increasing x, reflecting the evolution towards pure Fe^{3+} states.

ACKNOWLEDGEMENTS

The authors wish to thank Dr. V. A. M. Brabers (Techn. Univ., Eindhoven) for kindly providing the single crystals. They are thankful to Dr. D. Gryffroy and Mr. A. Van Alboom for helpful and stimulating discussions. This research was supported by the Fund for Joint Basic Research, Belgium (Grant No. 20055.87) and by the National Fund for Scientific Research, Belgium (Research Grant No. 31567289).

---

*Present address: Research Group Materials, Vlaams Instituut voor Technologisch Onderzock (V.I.T.O.), B-2400 Mol, Belgium.

[1]R. M. Persoons and E. De Grave, Solid State Commun. **72**, 977 (1989).

[2]R. Leyman, Ph.D. thesis, Gent State University, 1987.

[3]M. Rosenberg and H. Franke, in *Ferrites: Proceedings of the International Conference on Ferrites,* edited by H. Watanabe, S. Iida, and M. Sugimoto (University of Tokyo Press, Tokyo, 1981), pp. 146-148.

[4]J. Delepine, B. Hannoyer, F. Varret, and M. Lenglet, Hyperfine Interact. **28**, 721 (1986).

[5]B. Hannoyer, M. Lenglet, and J. C. Tellier, Rev. Chim. Miner. **24**, 68 (1987).

[6]G. A. Sawatzky, F. van der Woude, and A. H. Morrish, J. Appl. Phys. **39**, 1204 (1968).

[7]M. K. Fayek and A. A. Bahgat, Z. Phys. B **46**, 199 (1982).

[8]A. Stephenson, Philos. Mag. **25**, 1213 (1972).

[9]C. Zener, Phys. Rev. **82**, 403 (1951).

[10]H. Franke and M. Rosenberg, J. Magn. Magn. Mater. **4**, 186 (1977).

[11]H. Franke and M. Rosenberg, Physica **86-88B**, 965 (1977).

[12]H. Franke, M. Rosenberg, T. E. Whall, and M. R. B. Jones, J. Magn. Magn. Mater. **6**, 151 (1977).

[13]H. Franke, M. Rosenberg, T. E. Whall, and M. R. B. Jones, J. Magn. Magn. Mater. **7**, 223 (1978).

[14]H. Franke and M. Rosenberg, J. Magn. Magn. Mater. **9**, 74 (1979).

[15]M. Rosenberg, S. Dey, P. Deppe, and T. E. Whall, *Ferrites: Proceedings of the International Conference on Ferrites* (Ref. 3), pp. 101-105.

[16]M. Rosenberg, P. Deppe, H. U. Janssen, V. A. M. Brabers, F. S. Li, and S. Dey, J. Appl. Phys. **57**, 3740 (1985).

[17]D. D. Amarasiriwardena, E. De Grave, L. H. Bowen, and S. B. Weed, Clays Clay Minerals **34**, 250 (1986).

[18]P. M. A. de Bakker, R. E. Vandenberghe, and E. De Grave (unpublished).

[19]P. W. Anderson, Phys. Rev. **102**, 1008 (1956).

[20]R. Ingalls, F. van der Woude, and G. A. Sawatzky, in *Mössbauer Isomer Shifts,* edited by G. K. Shenoy and F. E. Wagner (North-Holland, Amsterdam, 1978), pp. 361-429.

[21]N. M. Gumen, Zh. Eksp. Teor. Fiz. **49**, 361 (1965) [Sov. Phys. JETP **22**, 251 (1966)].

[22]G. A. Sawatzky, F. van der Woude, and A. H. Morrish, Phys. Rev. **183**, 383 (1969).